Burn severity and vegetation type control phosphorus concentration, molecular composition, and mobilization

Morgan E. Barnes[1], J. Alan Roebuck, Jr[2], Samantha Grieger[2], Paul J. Aronstein[3], Vanessa A. Garayburu-Caruso[1], Kathleen Munson[2], Robert P. Young[1], Kevin D. Bladon[4], John D. Bailey[4], Emily B. Graham[1,5], Lupita Renteria[1], Peggy A. O'Day[3], Timothy D. Scheibe[1], Allison N. Myers-Pigg[2,6]

1 Pacific Northwest National Laboratory, Richland, WA, USA
2 Pacific Northwest National Laboratory, Sequim, WA, USA
3 Environmental Systems, University of California - Merced, Merced, CA, USA
4 College of Forestry, Oregon State University, Corvallis, OR, USA
5 School of Biological Sciences, Washington State University, Pullman, WA, USA
6 Department of Environmental Sciences, University of Toledo, Toledo, OH, USA

Correspondence to:
Allison Myers-Pigg (allison.myers-pigg@pnnl.gov)
Morgan Barnes (morgan.barnes@pnnl.gov)

Present Addresses:
Robert P. Young – Washington River Protection Solutions, P.O. Box 850 MSIN M0-01, Richland, WA 99354

Abstract

Shifting phosphorus (P) dynamics after wildfires can have cascading impacts from terrestrial to aquatic environments. However, it is unclear if shifts in P composition or P concentration are responsible for changes in P dynamics post-fire. We used laboratory leaching experiments of Douglas-fir forest and sagebrush shrubland chars to examine how the potential mobility of P compounds is influenced by different burn severities. Burning produced a 6.9- and 29- fold increase in particulate P mobilization, but a 3.8- and 30.5- fold decrease in aqueous P released for Douglas-fir forest and sagebrush shrubland, respectively. The mechanisms driving particulate and dissolved phase P compound mobilization were contrasting. Phosphorus compound mobilization in the particulate phase was controlled by solid char total P concentrations while the aqueous phase was driven by solubility changes of molecular species. Nuclear magnetic resonance and X-ray absorption near edge structure on the solid chars indicated that organic orthophosphate monoester and diester species were thermally mineralized to inorganic P moieties with burning in both vegetation types, which decreases P solubility. This coincided with the production of calcium- and magnesium-bound inorganic P compounds. With increasing burn severity there were systematic shifts in P concentration and composition— higher severity chars mobilized P compounds in the particulate phase, although the magnitude of change was vegetation specific. Our results indicate a post-fire transformation to both the composition of the solid charred material and to how P compounds are mobilized, which may influence its environmental cycling and fate.

47
48   **Short Summary**
49
50   Wildfires impact nutrient cycles on land and in water. We used burning experiments to
51   understand the types of phosphorous (P), an essential nutrient, that might be released to the
52   environment after different types of fires. We found the amount of P moving through the
53   environment post-fire is dependent on the type of vegetation and degree of burning which may
54   influence when and where this material is processed or stored.
55

56   **1 Introduction**

57   Wildfires are a major modifier of the terrestrial landscape, directly burning around 4% of the
58   Earth's surface each year (Randerson et al., 2012). They affect both the terrestrial and adjacent
59   aquatic environments and, as such, are considered one of the largest drivers of aquatic
60   impairment (Ball et al., 2021). Organic and inorganic nutrient pools and fluxes can be altered by
61   burning through multiple mechanisms. These include the loss of volatile compounds, altered
62   physiochemical properties from the incomplete combustion of organic material (from partially
63   charred biomass to ash; collectively referred to as chars (Bird et al., 2015), and enhanced
64   material transport from leaching and erosion (Bodí et al., 2014). The degree to which wildfires
65   impact ecosystems, or burn severity, is determined by the extent of organic matter loss or change
66   after fire and is influenced by fire intensity, heating duration, degree of live or dead plant
67   material, and fuel moisture, among other factors (Keeley, 2009). Fire frequency, intensity,
68   severity, and total area burned are expected to increase in many regions, such as the western
69   United States (Doerr and Santín, 2016; Haugo et al., 2019; Jolly et al., 2015). In particular, in the
70   Pacific Northwest, USA, burn severity and total burn area have increased in recent decades
71   (Francis et al., 2023; Halofsky et al., 2020; Reilly et al., 2017; Roebuck et al., 2024). Therefore,
72   it is important to understand the mechanisms behind how wildfires alter nutrient quantity,
73   composition, and mobilization.

74   Phosphorus (P; occurring primarily as orthophosphate $H_2PO_4^-$, HPO_4^{2-}, or PO_4^{3-}) is an essential
75   element (Smil, 2000) and is often a limiting nutrient to productivity in terrestrial and aquatic
76   environments (Elser et al., 2007). Ecosystem responses post-fire can include shifting terrestrial
77   nutrient acquisition by decreasing phosphatase activity and promoting net primary production
78   (Dijkstra and Adams, 2015; Saa et al., 1993; Vega et al., 2013). Phosphorus-containing
79   compounds transported to aquatic environments can also increase aquatic productivity,
80   influencing invertebrate and fish size and growth rate (Silins et al., 2014). While there is largely
81   an agreement across studies that P becomes enriched in chars after wildfire (Butler et al., 2018;
82   Elliott et al., 2013; García-Oliva et al., 2018; Schaller et al., 2015), with increased concentrations
83   in mineral soil (Butler et al., 2018) and river systems following wildfire (Lane et al., 2008;
84   Mishra et al., 2021; Rust et al., 2018), we are lacking a systematic understanding on how
85   variable burning conditions mediate the P concentration of charred organic material, and the role
86   of different fire-prone vegetation types (but see (Schaller et al., 2015; Wu et al., 2023b;
87   Yusiharni and Gilkes, 2012)) on availability for mobilization. Prescribed burns and wildfires
88   occur across a range of burning conditions (Merino et al., 2019; Santín et al., 2018; Vega et al.,
89   2013), which results in a mosaic of post-fire ecosystem responses on the landscape (Keeley,

90 2009). Therefore, understanding how P biogeochemistry is altered along a burn gradient will
91 provide insights on heterogenous responses observed across burned landscapes.

92 In the environment, P is found in multiple molecular moieties (i.e., orthophosphate, phosphonate,
93 orthophosphate monoester, orthophosphate diester, polyphosphate; orthophosphate monoester
94 and orthophosphate diester compound classes, referred to as the ester bonds moving forward)
95 which exist in different chemical states (i.e., adsorbed on surfaces, incorporated into minerals,
96 precipitated with metals). Chemical speciation influences the solubility and mobility of P, which
97 in turn impacts its bioavailability (Li and Brett, 2013; Turner et al., 2003b; Weihrauch and Opp,
98 2018; Yan et al., 2023). For example, bonding energy, or strength of the bonds, of the chemical
99 species generally increases from organic P to sorbed and mineral bound P species (Weihrauch
100 and Opp, 2018). The fate of these P species is determined by biological, chemical, physical, and
101 environmental factors, which vary in space and time (Condron et al., 2015; Yan et al., 2023).
102 Thus, the potential influence of wildfire effects on P dynamics and ecosystem productivity
103 cannot be adequately ascertained by only characterizing P concentration. Compared to changes
104 in total P concentration (i.e. the measure of all P compounds), there is less understanding of P
105 molecular composition in charred material and the impact this has on its mobilization (Robinson
106 et al., 2018; Wu et al., 2023a). As such, it is unclear if P biogeochemical responses post-fire are
107 due to changing composition of the charred material (i.e., composition controlled) and/or an
108 artifact of how P compounds are transported (i.e., mobilized from the solid char to then be
109 transported through the environment). Recent research on laboratory-produced plant-derived
110 chars has demonstrated the use of NMR to quantify P moiety (Sun et al., 2018; Uchimiya and
111 Hiradate, 2014; Wu et al., 2023b; Xu et al., 2016; Yu et al., 2023) and XANES to identify
112 chemical state (Robinson et al., 2018; Rose et al., 2019; Wu et al., 2023a; Yu et al., 2023). Taken
113 together, these complementary techniques are useful tools to provide a holistic understanding of
114 P molecular composition and can help to determine the environmental fate, as certain compounds
115 are preferentially volatilized, produced, and transported across the landscape (Son et al., 2015).

116 Vegetation burn severity is a common metric to describe how wildfires impact ecosystems
117 following a fire which allows for a post-fire assessment of ecosystem impacts (Keeley, 2009).
118 However, relatively few studies relate burn severity to fire effects on P biogeochemistry (Souza-
119 Alonso et al., 2024; Vega et al., 2013) even though it is a more commonly used field metric than
120 fire intensity because it can be measured after the burn (Zavala et al., 2014). Thus, burn severity
121 allows for field relevant understanding how burning conditions beyond the impact of temperature
122 alone. Experimental studies along burn severity gradients provide an opportunity to better
123 understand field conditions post-fire. To understand the amount and types of materials derived
124 from plant litter that could be transported from terrestrial to aquatic systems along a burned
125 gradient, we examined how P concentration and molecular composition in solid chars and their
126 leachates vary across a burn severity gradient. We hypothesize that changing P composition in
127 the solid charred materials with increasing burn severity will influence the leachability of P
128 compounds in the particulate and aqueous phases, and this will be moderated by vegetation
129 type. To test this hypothesis and better understand the amount and types of materials that could
130 be mobilized along a burned gradient, we examined how burn severity influences P
131 concentration and molecular composition in experimentally generated solid chars and their
132 leachates from two common vegetation types present in the Pacific Northwest.
133
134 **2 Materials and Methods**

135 All datasets and detailed methodology used in this manuscript are available from Grieger et al.
136 (Grieger et al., 2022) version 3 and Barnes et al. (Barnes et al., 2024) on the Environmental
137 System Science Data Infrastructure for a Virtual Ecosystem (ESS-DIVE) repository.

138 *2.1 Burn Experiments*

139 Vegetation was collected from two fire-prone landscapes of contrasting vegetation types to
140 represent archetypes of vegetation commonly found in the Pacific Northwest, USA that also have
141 differing wildfire characteristics (Halofsky et al., 2020; Reilly et al., 2017; Roebuck et al., 2024;
142 Stavi, 2019). In this study, we chose to explore vegetation that is representative of Douglas-fir
143 forests (*Pseudotsuga menziesii*), which tend to burn in the environment at higher intensities, and
144 sagebrush shrublands (*Artemisia tridentata*), which tend to burn at lower intensities (Stavi,
145 2019). Samples were chosen to be representative of possible living vegetation and litter materials
146 of the dominant species from these landscapes (Grieger et al., 2022; Myers-Pigg et al., 2024;
147 Roebuck et al., 2024). Exact site locations and sampling details can be found in our
148 accompanying data package (Grieger et al., 2022). For Douglas-fir, a mix of living and dead
149 material was collected, while sagebrush was in partial senescence upon collection. All plant
150 materials were air dried for at least two weeks before burning. Woody and canopy materials were
151 mixed at a known ratio (40% materials < 0.5 cm and 60% materials > 0.5 cm) before each burn,
152 and this was held constant for each burn (Grieger et al., 2022).
153
154 Chars were generated using an open air burn table, as biochars produced in laboratories have
155 been found to be compositionally different than chars generated in open air burns and wildfires
156 (Myers-Pigg et al., 2024; Santín et al., 2017). To create burns that would result in a range of
157 vegetation burn severities, we manipulated fire behavior on the burn tables by varying burn
158 temperature, duration of heating, fuel moisture content (by experimentally adding moisture to
159 dried materials), fuel density, and vegetation status (i.e., living or litter). Thermocouples were
160 used to monitor temperature over the burn duration, and char grab samples were targeted for 300
161 °C, 600 °C, and when flames and smoldering commenced (sagebrush shrubland burns did not
162 reach 600 °C). Char burn severity was visually classified as low, moderate or high following US
163 Forest Service field metrics based on ash color, degree of consumption, and degree of char
164 (Grieger et al., 2022; Parsons et al., 2010) (Fig. S1). Thus, burn severity was determined by the
165 extent of organic matter loss or change after fire and is influenced by fire intensity, heating
166 duration, degree of live or dead plant material, and fuel moisture, among other factors and is not
167 a measure of fire intensity (the amount of energy released from a fire) nor burn temperature,
168 though it is related to both (Keeley, 2009). The characterization of burn severity results in
169 overlapping maximum temperatures of several of the assigned burn severity categories in our
170 results.

171 Unburned samples and chars were air dried; subsamples were finely ground for elemental
172 composition and were stored in the dark at room temperature until further analysis.

173 *2.2 Elemental Analysis of Solid Samples*

174 Total P, sulfur (S), aluminum (Al), iron (Fe), magnesium (Mg), calcium (Ca), sodium (Na), and
175 potassium (K) were measured using an inductively coupled plasma optical emission
176 spectrometer (ICP-OES) model Optima 7300 DV (PerkinElmer, Waltham, MA). Solid samples
177 were digested with aqua regia at 130 °C for 8 h in an incubation oven (ThermoFisher Scientific,
178 Waltham, MA).

179   For samples that underwent NMR analysis, approximately 0.5 g of finely ground sample was
180   extracted in a 10 mL solution of 0.25 M NaOH and 0.05 M EDTA for 16 h, followed by
181   centrifugation, filtration, and measurement on ICP-OES (Sun et al., 2018; Turner et al., 2003b).
182   The goal of the NaOH-EDTA extraction is to get the maximum amount of P into solution.
183   Extraction efficiencies are reported in Table S1 (see SI section Method Limitations for additional
184   information).

185   *2.3 Solution ^{31}P NMR on Solid Samples*

186   After aliquoting 3 mL of the NaOH-EDTA extracts for ICP-OES, the remaining supernatants
187   were frozen and lyophilized to concentrate the extracted compounds. Immediately prior to
188   running NMR experiments (Environmental Molecular Science Laboratory; EMSL, Richland,
189   WA), freeze-dried extracts were reconstituted in 0.52 mL deuterium oxide (D_2O) and 0.26 mL of
190   10 M NaOH, and 0.52 mL of a solution containing 0.5 M NaOH and 0.1 M EDTA. Full
191   experimental ^{31}P NMR measurement details are provided in the supporting information. In brief,
192   NMR measurements were conducted on an Agilent DD2 spectrometer operating at a field
193   strength of 14.1T (242.95 MHz ^{31}P), equipped with a 5mm Varian broadband direct detect probe.
194   Experiments were conducted at a regulated temperature of 20.0°C. A standard 1D pulse and
195   acquire experiment was performed using a 90° pulse width and recycle delay equal to 5 × T1,
196   which were calibrated and measured individually for each sample using the orthophosphate peak
197   present in each. Samples were measured for 16 h each with the number of transients acquired
198   dependent upon T1 for each individual sample. Post-acquisition processing and analysis was
199   performed using Mnova 14.0.1 (Mestrelab Research, Spain). Details regarding classification of
200   major P forms, identification of specific P compounds from spiking experiments, quantitation,
201   and method limitations are described in detail in the supporting information (Cade-Menun, 2015;
202   Doolette et al., 2009; Recena et al., 2018) (Fig. S2).

203   *2.4 Solid Sample P XANES*

204   X-ray absorption near edge structure (XANES) is a complementary technique to solution ^{31}P
205   NMR because it can discern the complexation environment of P in solid samples (see SI section
206   Method Limitations for additional information). Bulk XANES was conducted on beamline 14-3
207   at the Stanford Synchrotron Radiation Lightsource (SSRL, Stanford, CA). The beamline was
208   calibrated at the P K-edge with the first peak of tetraphenylphosphonium bromide at 2146.96
209   eV.

210   Sample spectra were fit using least-squares linear combination in Athena (Ravel and Newville,
211   2005) (Fig. S3). Baseline correction and edge-step normalization parameters were varied for
212   individual samples and reference compounds to reduce error (Werner and Prietzel, 2015). Fits
213   were performed with the component sum not forced to unity, a maximum of three reference
214   compounds, and only fits within ± 2.5% were used. If a component fit < 5%, then this reference
215   compound was removed, and the sample was refit with the remaining compounds. The R-factor
216   of all sample fits were < 0.05 (Table S2), indicating a good quality of fit (Kelly et al., 2015). Fits
217   were performed with a variety of Ca, Al, Fe, Mn, K, and Na inorganic and organic P-containing
218   reference compounds. Individual inorganic P compounds (P_i; includes phosphate and
219   pyrophosphate moieties) reference compounds were grouped based on the associated metal and
220   all organic P compounds (P_o; includes monoester and diester moieties) were kept as a separate
221   category (Fig. S3; Table S3). Additional information on sample preparation, linear combination

222 fits, reference compounds, and method limitations are described in the supplemental information
223 (XANES Methodology section).

2.5 Leaching Experiments

225 Leachates from unburned material and char samples were generated in triplicate. Briefly, 25 g of
226 unground sample was shaken in the dark for 24 h in 1000 mL of synthetic rainwater (pH ~ 5) to
227 simulate what might be mobilized by rain events from the solid material and subsequently
228 transported from terrestrial to aquatic environments (Grieger et al., 2022). Our starting mass was
229 kept constant to understand differences in the amounts of materials leached across burn severity
230 gradients, and so our results are directly comparable to temperature gradient studies (Bostick et
231 al., 2018). Therefore, leaching experiments had a different goal of simulating natural
232 mobilization of P compared to the NMR extractions, where we tried to maximize P extracted.
233 Leachates were filtered through a PTFE mesh (2 mm x 0.6 mm) followed by a pre-combusted
234 GF/F filter (< 0.7 µm). Aliquots were immediately taken for subsequent analysis and preserved
235 according to analytical needs described below.

2.6 Elemental Analysis of Leachates

237 Coarse filtered (< 2 mm) and < 0.7 µm filtered (i.e., aqueous phase) leachates were preserved in
238 1% nitric acid and stored at 4 °C until analysis. Aliquots of 5 mL were transferred to 15 mL
239 centrifuge tubes, acidified to 10% (v/v) trace metal grade hydrochloric acid and 4% (v/v) trace
240 metal grade nitric acid. Tubes were fully sealed and heated at 85 °C for 2.5 h in an incubation
241 oven (ThermoFisher Scientific, Waltham, MA) and then total elemental analysis were measured
242 by ICP-OES. Total P of the leachate particulate phase (2 mm to 0.7 µm) was calculated as the
243 difference between the coarse filtered and aqueous phase.

244 Molybdate reactive P was determined on aqueous phase leachate aliquots preserved in 0.2%
245 sulfuric acid and stored at 20 °C, following EPA method 365.3 (Method 365.3: Phosphorus, All
246 Forms (Colorimetric, Ascorbic Acid, Two Reagent)). Aqueous non-molybdate reactive P was
247 calculated as the difference between aqueous total P (as measured by ICP-OES) and molybdate
248 reactive P.

2.7 Data Analyses

250 Leachable P (mg g P^{-1}; particulate and aqueous phases separately) was calculated by normalizing
251 to the P concentration of the solid samples following Equation 1 (Fischer et al., 2023):

$$Leachable\ P_{particulate\ or\ aqueous} = \frac{leachate\ P\ (mg\ L^{-1})\ x\ leaching\ volume\ (L)}{mass\ of\ dry\ char\ (g)\ x\ P\ content\ of\ dry\ char\ (mg\ P\ g^{-1})}$$

253 All statistical tests were conducted in R version 4.2.3 (R Core Team, 2023). Data calculations,
254 statistical analyses, and figures are freely available (Barnes et al., 2024). For all statistical
255 analyses, model assumptions were assessed with a Shapiro-Wilk test of normality using the
256 package stats (R Core Team, 2023) and spread-location plots to inspect homoscedasticity. All
257 analyses met assumptions after log transformation. Significance was determined at the $\alpha = 0.05$
258 level. All data are reported as the mean ± standard deviation unless otherwise stated.

259 Separate analysis of variance (ANOVA) models were used to test how burn severity, vegetation
260 type, and their interaction influences solid P concentration. For leachate samples (i.e., particulate
261 total P, aqueous total P, aqueous molybdate reactive P), mixed-effect models were run with the

262   same fixed effects as the solid samples and a random effect was used to account for triplicate
263   leachates produced from the same solid sample. Mixed effect models were performed with the
264   lme4 package (Bates et al., 2015) and were fit by maximum likelihood. Variance Inflation
265   Factors were used to inspect for multi-collinearity of fixed effects with the car package (Fox and
266   Weisberg, 2018). Post-hoc pairwise comparisons were conducted using least squares means in
267   the emmeans package (Lenth, 2023). These data are presented in boxplots, which denote the first
268   and third quartiles as the lower and upper hinges, while the whiskers are the largest and smallest
269   values up to 1.5 times the interquartile range. Outliers are captured as individual points on the
270   boxplots, as they are outside the whiskers.

271   Path analysis was conducted to analyze the hypothesized relationships that may explain how
272   burn severity and vegetation type influence P compound mobilization (i.e., leachable particulate
273   or aqueous phase P concentration) indirectly through changes in char conditions (i.e., P
274   concentration and chemical composition). Calcium-bound P_i was used as a proxy for chemical
275   composition because it is a primary control of P compound solubility in charred materials
276   (Schaller et al., 2015; Uchimiya and Hiradate, 2014; Wu et al., 2023b; Yu et al., 2023).
277   Phosphorus compound mobilization was estimated as the average leachable P from the parent
278   solid samples. Models were run with the sem package (Fox, 2006), with burn severity and
279   vegetation type directly impacting the P concentration and proportion of Ca- P_i in the solid
280   samples, which in turn influence the leachable P concentration. Vegetation type is also set up to
281   directly impact burn severity (Fig. S4).

282   **3 Results and Discussion**

283   *3.1 The magnitude of char P increase with burn severity depends on vegetation type*

284   In our study, using experimental open air burns, we found total P concentration (measured using
285   ICP-OES) increased with burn severity in both Douglas-fir forest and sagebrush shrubland solid
286   samples (Fig. 1). Our findings were consistent with observations of increasing P concentration
287   from laboratory-produced chars (García-Oliva et al., 2018; Zheng et al., 2013) and in chars
288   collected shortly after wildfire and prescribed burns (Butler et al., 2018). In particular, while our
289   burn treatments did not reach temperatures that would result in P volatilization, they did
290   represent heterogenous burn conditions, incorporating a variety of burn durations and
291   temperature ranges (Grieger et al., 2022; Myers-Pigg et al., 2024) that are consistent with other
292   open air burn experiments (Brucker et al., 2022, 2024) (Table 1; Fig. S1). The P concentration in
293   unburned Douglas-fir forest samples was 1.3 ± 0.5 g P kg^{-1} and increased to an average of $6.2 \pm$
294   1.9 g P kg^{-1} in high-severity burns (ANOVA post hoc $p < 0.001$). On the other hand, unburned
295   sagebrush shrubland material contained 1.3 g P kg^{-1} compared to 14.5 ± 3.5 g P kg^{-1} in the
296   moderate-severity burns (ANOVA post hoc $p < 0.001$), the highest severity classes reached for
297   each vegetation type. The observed increase in char P indicated that retention (i.e., condensation)
298   outweighed loss via volatilization. Generally, P and metal cations volatilize at higher
299   temperatures (774 °C or greater) than carbon (C) and nitrogen (N) (>200 °C), so they are often
300   retained in charred material rather than lost in gaseous form (Son et al., 2015). Therefore, our
301   study may underestimate P transformations linked to P volatilization from burns that reach
302   higher temperatures than our experimental burns.
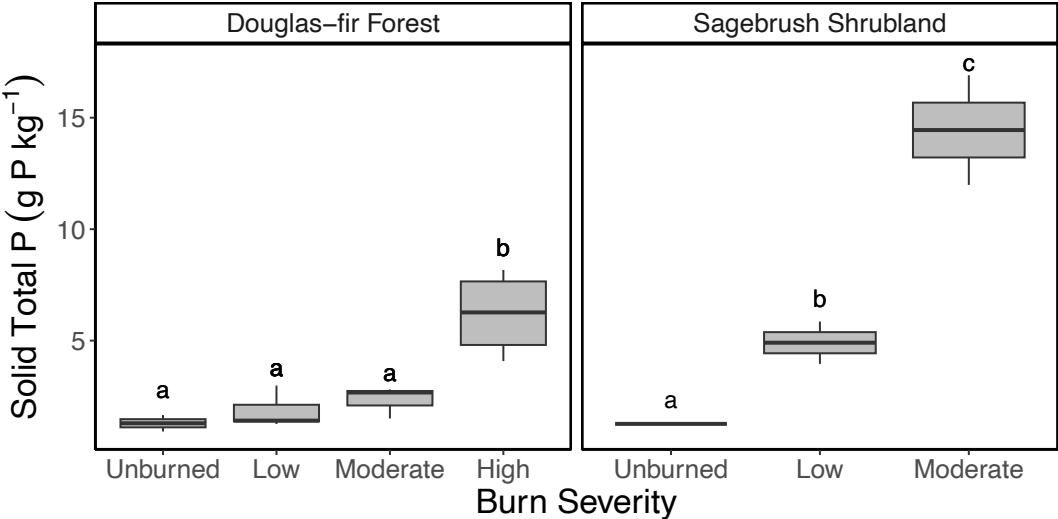
303

Figure 1. Boxplot of P concentration (g P kg^{-1}) in the solid samples along Douglas-fir Forest and Sagebrush shrubland burn severity gradients. Letters denote post hoc findings of burn severity significant differences within a vegetation type, where the same lettering indicates no significant difference. See Table 1 for burn duration, temperature, and sample size.

304   Although P concentration in solid samples increased from unburned to the highest burn severity
305   classification reached in both vegetation types, the magnitude was vegetation dependent
306   (ANOVA interaction term: F = 6.23, p = 0.014). In Douglas-fir forest chars, P concentration was
307   unchanged by burning until high burn severity was reached (post hoc test; low: p = 0.658,
308   moderate: p = 0.277, high: p < 0.001), while P in sagebrush shrubland chars increased even after
309   low burn severity (post hoc test; low: p = 0.034, moderate: p < 0.001). Post hoc tests further
310   identified that the P concentration of sagebrush shrubland chars was significantly greater than
311   Douglas-fir forest within the same burn severity classification (low: p = 0.0038; moderate: p <
312   0.001), even though unburned samples were not statistically different (p = 0.962). On average,
313   total P in sagebrush shrubland chars were 2.7 and 6.2 times higher than Douglas-fir forest in low
314   and moderate-severity burns, respectively (Fig. 1).

315   Remarkably, P in moderate-severity sagebrush shrubland chars was even higher than Douglas-fir
316   forest high-severity chars; these represent the highest burn severity observed for each vegetation
317   type. Higher maximum char temperatures or burn duration does not explain why P concentration
318   is greater in burned sagebrush shrubland material compared to Douglas-fir forest; sagebrush
319   shrublands experienced lower maximum temperatures (530 ± 25 °C) and shorter burn duration
320   (202 ± 3 minutes) in moderate-severity burns compared to Douglas-fir forest high-severity burns
321   (704 ± 78 °C; 783 ± 195 minutes; Table 1).

322

323

324

Burn Severity	Vegetation	Burn Duration (Minutes)	Lowest Max Temp (°C)	Highest Max Temp (°C)	n solids	n leachates
Unburned	Douglas-fir forest	NA	25	25	2	6
	Sagebrush shrubland	NA	25	25	1	3
Low	Douglas-fir forest	342 (403)	295	627	5	15
	Sagebrush shrubland	131 (104)	308	512	2	6
Moderate	Douglas-fir forest	456 (303)	589	757	3	9
	Sagebrush shrubland	202 (3)	512	547	2	6
High	Douglas-fir forest	783 (195)	589	757	4	12

325 Table 1. Burn characteristics for severity classifications for each vegetation type including mean
326 (standard deviation) duration, low and high range of maximum temperature reached during burn
327 duration, and count of the solid and leachate samples.
328
329 One mechanism that could explain such results is that sagebrush shrublands may be composed of
330 volatile organic compounds that are more susceptible to loss compared to Douglas-fir forests,
331 leading to selective enrichment of P compounds relative to Douglas-fir forest chars. However,
332 emission factors and total volatile organic compounds from sagebrush and coniferous fuels are
333 relatively similar (Hatch et al., 2019; McMeeking et al., 2009). This suggests that the observed
334 enrichment of sagebrush shrubland P with burning may be due to differences in the conversion
335 of organic P to inorganic P in the sagebrush shrubland materials, which can arise from different
336 fire conditions (Fiddler et al., 2024). Sagebrush shrublands may be more susceptible to changing
337 P dynamics post-fire because chars are likely enriched in P to a greater extent than Douglas-fir
338 forests, even at low severities.

339 *3.2 Solid char molecular composition is influenced by burn severity and vegetation type*

340 Organic P in the solid char was progressively transformed to inorganic species across both
341 vegetation types. Unburned Douglas-fir forest and sagebrush shrubland had similar initial
342 percentages of total organic P with $40.5 \pm 3.3\%$ and 53.7%, respectively (identified by NMR
343 extracts, Fig. 2; also supported by XANES on solid phase, Fig. 3). As burning progressed, the
344 total organic P pools reduced to only $12.6 \pm 8.2\%$ for Douglas-fir forest and $10.4 \pm 8.4\%$ for
345 sagebrush shrubland low-severity chars. While organic P moieties were still present in Douglas-
346 fir forest chars produced at moderate severities ($4.4 \pm 4.2\%$), $<1\%$ was measured in sagebrush
347 shrubland. Moderate-severity sagebrush shrubland chars more closely resembled high-severity
348 Douglas-fir forest with nearly all organic P moieties lost ($<1\%$). This further supports the
349 conclusion that different fire conditions were experienced by Douglas-fir forest and sagebrush
350 shrubland in our simulated burns. Although it has been suggested that organic P can be fully
351 transformed to inorganic species at 200 °C (García-Oliva et al., 2018), another study of organic
352 horizons found organic P moieties persisted after low, moderate, and high-severity fires that
353 reached up to 872 °C (Merino et al., 2019). We measured organic P in burns that reached above
354 600 °C, suggesting that the thermal mineralization of organic to inorganic P compounds is

355   controlled by microscale differences in temperature and selective physical protection (i.e.,
356   mineral aggregates) rather than what is observed at overall bulk temperatures, and is likely a
357   result of the interaction between temperature, burn duration, and vegetation type experienced by
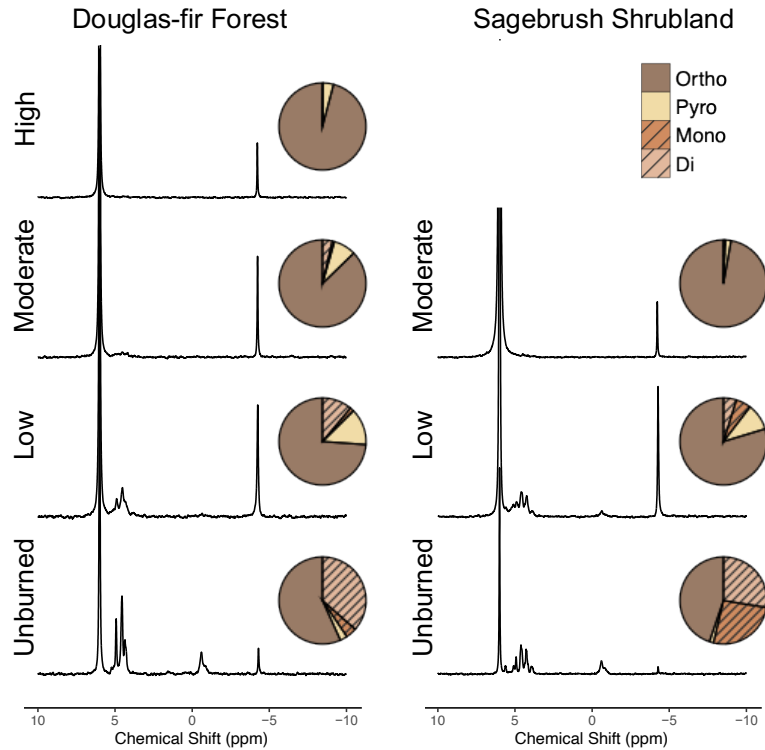358   these microsites (Galang et al., 2010; Lopez et al., 2024).

Figure 2. Solution ^{31}P nuclear magnetic resonance (NMR) spectra from a
representative solid char sample of each burn severity and vegetation type.
The number of scans varied for each sample, based on relaxation time, and
therefore direct comparisons of peak intensities can only be made within a
spectrum (see additional details in SI NMR Methods). Averaged replicates
are represented by pie charts for the proportions of orthophosphate (ortho),
pyrophosphate (pyro) monoesters (mono) and diesters (di). Orthophosphate
and pyrophosphate are inorganic species (brown colors) and monoester and
diesters are organic species (orange colors with hashed lines). See SI
sections NMR Methodology and Method Limitations for additional details
and Table 1 for burn duration, temperature, and sample size.

359   Previous studies have suggested charred materials containing diester species (two C moieties per
360   P) are more vulnerable to thermal mineralization than monoesters (one C moiety per P) (García-
361   Oliva et al., 2018; Turrion et al., 2010). However, we found diester and monoester species
362   followed similar proportional decreases in our chars with burning (Fig. S5). Hence, both readily
363   available (i.e., diester) and less labile (i.e., monoester) organic P species (Condron et al., 2015)
364   were converted to inorganic P at comparable rates, which is similar to forest and shrubland
365   organic horizons subjected to prescribed fire (Merino et al., 2019). This suggests there is not a
366   fundamental molecular difference in how these moieties respond to burning in organic material

367 such as what is examined in our study, but instead the preferential loss of diesters in burned
368 mineral soil may be because the stronger sorption of monoesters to soil particles attenuates the
369 heat.

370 Because diester and monoester species were lost at similar proportions, the composition of the
371 unburned material dictated the resulting char P composition and potential bioavailability. Across
372 both vegetation types, we identified phospholipids, DNA, and RNA (diester region) and phytate
373 and sugar phosphates (monoester region; Fig. 2; Table S4), which follows other studies of
374 vegetation P composition (Doolette and Smernik, 2016; Noack et al., 2012). However, the
375 proportions of these species were vegetation dependent, where unburned Douglas-fir forest was
376 dominated by diesters (36.5 ± 9.1%) with minor percentages of monoesters (4.1 ± 5.7%),
377 whereas sagebrush shrubland was nearly equal parts diesters (27.6%) and monoesters (26.1%).
378 RNA, DNA, phospholipids, and sugar phosphates are considered bioavailable due to their weak
379 adsorption, whereas phytate strongly sorbs to both organic and inorganic particles making it
380 relatively less available for biological uptake (Condron et al., 2015; Li and Brett, 2013; Turner et
381 al., 2003a). Douglas-fir forest was composed of a greater proportion of these bioavailable
382 organic species in unburned (36.8 ± 7.6%) and low-severity burns (12.4 ± 8.4%) compared to
383 sagebrush shrubland (unburned: 32.4; low: 8.0 ± 4.5%).

384 With increased burn severity, Douglas-fir forest (high-severity) and sagebrush shrubland
385 (moderate-severity) organic speciation converged with only < 1% of organic P (as RNA)
386 remaining. Prior studies using NMR in plant-based biochar produced from 300 – 800 °C found
387 char was composed of entirely inorganic P, including orthophosphate (27–97%) and
388 pyrophosphate (3–71%; although one sample produced at 350 ˚C was 2% phospholipids) (Sun et
389 al., 2018; Uchimiya et al., 2015; Uchimiya and Hiradate, 2014). The unburned parent material in
390 these studies had variable starting compositions with organic P ranging from 3–87% (as phytate).
391 The extent of organic P loss in these studies is most similar to our higher severity samples, once
392 again demonstrating that factors beyond just temperature determines the composition of P in
393 charred material. Overall, these findings suggest organic P moieties in charred material are
394 determined by the degree of burning, where lower severity chars resemble the starting
395 composition, and this is influenced by vegetation type.

396 As organic species were thermally mineralized in our chars, inorganic P, such as pyrophosphate,
397 was produced (Fig. 2). Pyrophosphate can be produced either from orthophosphate or phytate
398 and is thought to largely originate from fungal tissue (Bünemann et al., 2008; Makarov et al.,
399 2005), although it has been found in some plants (Noack et al., 2012; Wu et al., 2023b). We
400 found pyrophosphate peaked in low-severity chars across both vegetation types, reaching 13.6 ±
401 3.1% in Douglas-fir forest and 9.9 ± 6.2% in sagebrush shrubland burns. Prior NMR studies on
402 plant chars produced between 350 - 800 °C have also observed an increase in the proportion of
403 pyrophosphate relative to unburned material, followed by a decrease at higher charring
404 conditions (Sun et al., 2018; Uchimiya and Hiradate, 2014). Variability in pyrophosphate from
405 naturally produced chars has also been observed. For example, post wildfire, pyrophosphate was
406 ~3% in a pine forest (García-Oliva et al., 2018), absent in a eucalyptus forest (Santín et al.,
407 2018), 0–13% of cedar-hemlock forests (Cade-Menun et al., 2000), and 3–7% from pine forests
408 and shrublands (Merino et al., 2019). Thus burned organic material, especially in chars produced
409 at low-severity wildfire and prescribed burns, may be an important, yet underappreciated, source
410 of pyrophosphate in the environment.

The production of pyrophosphate in our charred plant material is likely a result of the initial organic matter composition and burning conditions (Wu et al., 2023b; Yu et al., 2023). Pyrophosphate and other polyphosphates can be produced from orthophosphate during burning, with the thermal degradation of phytate (organic P; monoester) contributing more orthophosphate (Robinson et al., 2018; Rose et al., 2019; Uchimiya and Hiradate, 2014). Pyrophosphate was greater in Douglas-fir forest chars compared to sagebrush shrublands, even though sagebrush shrubland chars contained more phytate in the unburned material (Fig. 2). This indicates pyrophosphate was primarily produced from polymerization and dehydration of orthophosphate, and not from thermal degradation of phytate in our chars (Uchimiya and Hiradate, 2014).

Although pyrophosphate peaked in low-severity chars, we found the percentage of total inorganic P species continued to increase with burning across both vegetation types, as measured by NMR on solid extracts and XANES of intact solid samples (Fig. 2, Fig. 3; Tables S2 and S4), demonstrating additional transformations to P composition with increasing severity. Inorganic species, measured by XANES, in unburned material was composed largely of P compounds associated with Fe (37% sagebrush shrubland; $40 \pm 5\%$ Douglas-fir forest; fitting primarily as P_i sorbed to the surface of goethite) and a minor component of Ca-bound P_i species ($3 \pm 3\%$ Douglas-fir forest; 9% sagebrush shrubland; fitting mostly as apatite). The proportion of Ca- and Mg-P_i (fitting as magnesium phosphate and/or struvite) increased with burn severity (Fig. 3; Table S2). Douglas-fir forest high-severity chars had $52.8 \pm 8.3\%$ Ca-P_i and $29.0 \pm 9.9\%$ Mg-P_i, while sagebrush shrubland moderate-severity chars contained $45.1 \pm 0.1\%$ Ca-P_i and $53.7 \pm 0.1\%$ Mg-P_i.

Other studies using XANES supports the production of Ca-P_i, along with Fe- or Mg-P_i in plant-based chars and ash (Robinson et al., 2018; Sun et al., 2018; Uchimiya and Hiradate, 2014; Wu et al., 2023a), whereas studies using other techniques (solid-state NMR, sequential fractionation) have found higher temperatures result in greater Ca- and Al-P_i (García-Oliva et al., 2018; Xu et al., 2016). Hydroxyapatite and other stable forms of Ca-P_i minerals are known to be produced by organic matter combustion (Uchimiya and Hiradate, 2014), so it follows that these P species are produced with burning and progressively increase along our burn severity gradient. P compound bonding environments have been found to resemble stoichiometric ratios of the burned material (Wu et al., 2023a; Zwetsloot et al., 2015) .Our findings support this where Ca- and Mg-P_i species increased as the proportion of Ca and Mg also increased (Fig. 3; Tables S2, S5, and S6). Phosphorus mobility and bioavailability of P compounds are likely influenced by increased inorganic P proportions because Ca-P_i, especially apatite, is considered to have low water extractability and apparent bioavailability (García-Oliva et al., 2018; Li and Brett, 2013; Zwetsloot et al., 2015).
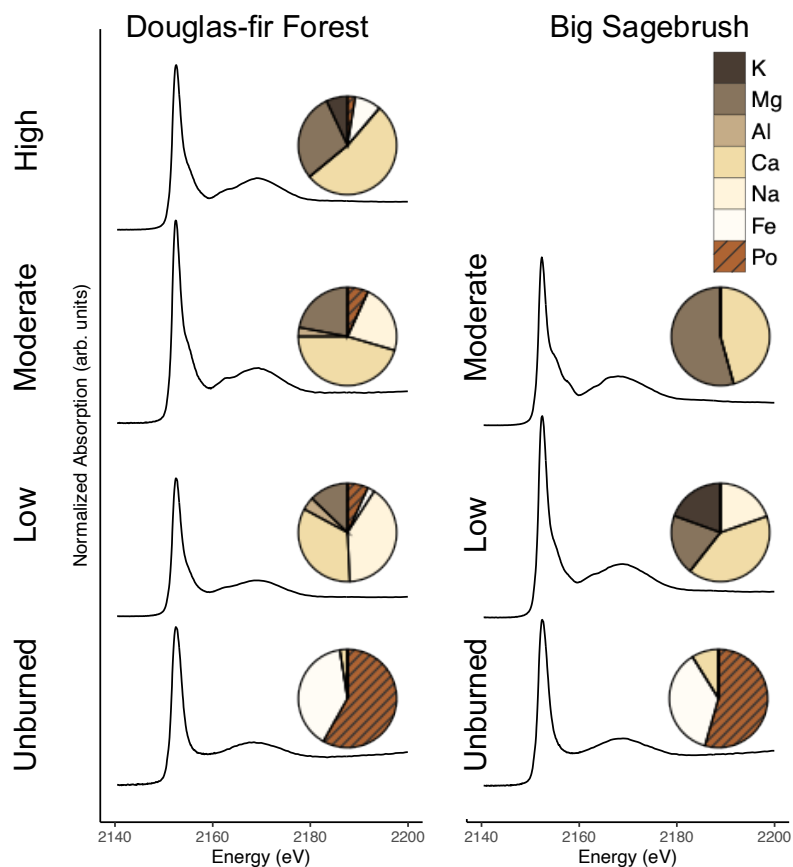
Figure 3. Phosphorus K-edge X-ray absorption near edge structure (XANES) spectroscopy from a representative solid unburned and char sample of each burn severity and vegetation type. Averaged replicates are represented by pie charts for the proportions of P_i associated with K-, Mg-, Al-, Ca-, Na-, and Fe (brown colors) and P_o species grouped together regardless of metal association (orange color with hashed lines; see SI XANES Methods for additional details). See SI sections XANES Methodology and Method Limitations for additional details and Table 1 for burn duration, temperature, and sample size.

447

3.3 Leachable particulate- and aqueous-bound P have contrasting mobilization patterns with burning and are under differing controls

As burn severity increased, the enriched P of the solid chars resulted in greater particulate P mobilized (assessed via leaching experiments), regardless of vegetation type ($\beta = 0.78$, $p <$ 0.001, $r^2 = 0.68$; Fig. 4, Fig. 5). Burning resulted in a 6.9- and 29- fold increase of particulate P mobilization from Douglas-fir forest (high-severity) and sagebrush shrubland (moderate-severity) chars, respectively (Fig. 4). Phosphorus compounds may be largely physically protected in the matrix of the charred material (70–90% residual P in sequential fractionation scheme (Wu et al., 2023b)), therefore it follows that particulate P patterns are controlled by changes in solid

13

char concentration; charred material becomes enriched with P and there is production of highly mobile particulates (such as ash (Blake et al., 2010)). Path analysis identified that burn severity ($\beta = 0.61$, $p < 0.001$) and vegetation type ($\beta = 0.65$, $p < 0.001$) had direct influence on solid char P concentration ($r^2 = 0.64$; Fig. 5). Mixed effect model results further demonstrate that the effect burn severity has on leachable particulate P is vegetation dependent (interaction term of mixed effect model; $p = 0.009$). Moderate-severity sagebrush shrubland chars mobilized 5.2 times more P in the particulate phase than Douglas-fir forest ($p = 0.04$). Particulate P mobilized from charred material can be transported to waterways, as a meta-analysis found unfiltered P concentrations in the western United States increased ~1.7 times after wildfire ($n = 46$) (Rust et al., 2018).
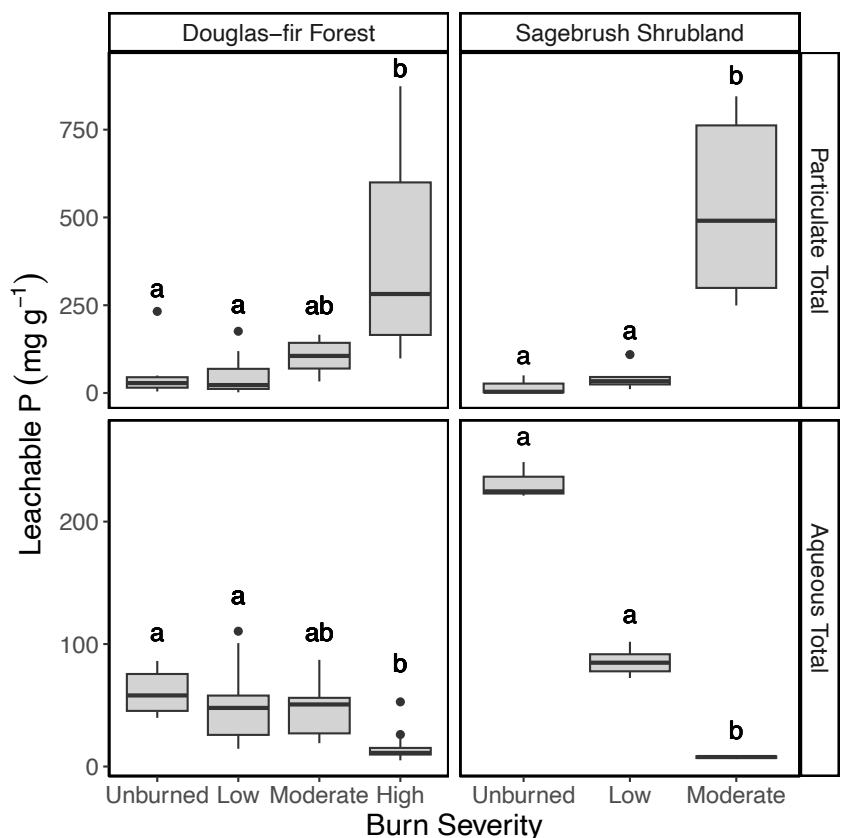
Figure 4. Boxplot of the relationship between burn severity and vegetation type with leachable P concentration (mg P g⁻¹; calculated from Equation 1) for total P in the particulate phase and total P in the aqueous phase. Molybdate-reactive P in the aqueous phase are reported in the SI. Letters denote post hoc findings of burn severity significant differences within a vegetation type, where the same lettering indicates no significant difference. Note difference scales of the y-axis for the particulate and aqueous phases. See Table 1 for burn duration, temperature, and sample size and Figure S6 for leachable aqueous molybdate reactive P results.
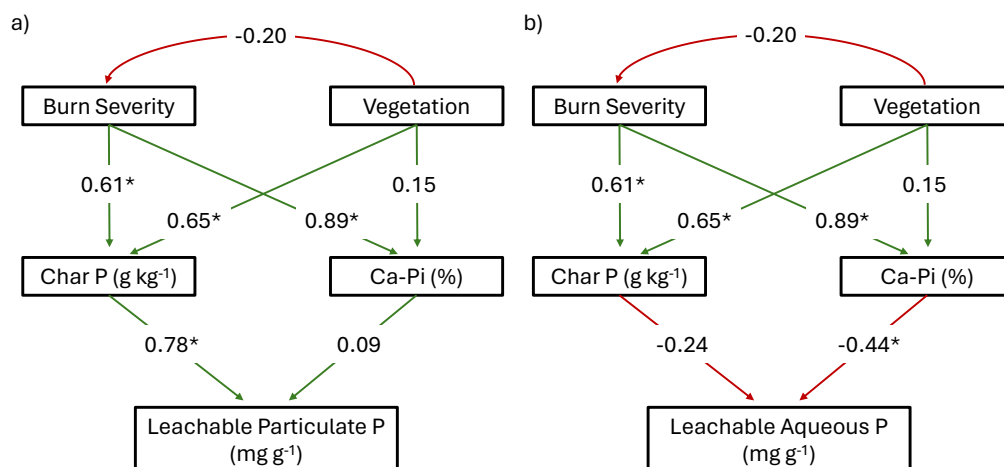
Figure 5. Path analysis model results for the impact of burn severity and vegetation type on leachable P in the (a) particulate and (b) aqueous phases, as mediated by solid unburn and char P concentration and chemical composition. All relationships are reported with significance ($\alpha = 0.05$) denoted with an asterisk symbol on the standardized correlation coefficient (analogous to relative regression weights). Paths are green for positive relationships and red for negative. Leachable Particulate P Model: $\chi^2 = 16.277$, $p < 0.05$, df = 3, RMSEA = 0.483, AIC = 108.3; Leachable Aqueous P Model: $\chi^2 = 19.032$, $p < 0.05$, df = 3, RMSEA = 0.530, AIC = 122.1. See Fig S4 for original hypothesized model.

466   In contrast to leachable particulate P, mobilization of P in the aqueous phase decreased 3.8-fold
467   for Douglas-fir forest and 30.5-fold for sagebrush shrubland with burning (Fig. 4). Prior work
468   from laboratory-produced plant chars have found decreased water-soluble P even though solid
469   char concentration increased with burning (Gundale and DeLuca, 2006; Mukherjee and
470   Zimmerman, 2013; Wu et al., 2011; Yu et al., 2023; Zheng et al., 2013). Instead of
471   concentration-controlled like particulate P, aqueous P mobilization was composition-controlled
472   (represented as percentage of Ca-P$_i$ in our path analysis, $\beta = -0.44$, $p = 0.041$, $r^2 = 0.34$; Fig. 5).
473   We chose to represent P composition in the path analysis as Ca-P$_i$ to simplify the path analysis
474   interpretation. In reality, drivers of aqueous P mobilization extend beyond Ca-P$_i$ and include
475   other compositional shifts, such as Mg-P$_i$, organic P speciation, and pH. Phosphorus compound
476   adsorption to multivalent cations (Ca^{2+}, Mg^{2+}, Fe^{3+}, and Al^{3+}) can decrease aqueous phase export
477   (Glaser et al., 2002). Indeed, we found higher severity burns had greater concentrations of metals
478   (Tables S5 and S6) which interacted with P to form primarily Ca- and Mg-P$_i$ species (Fig. 3;
479   Table S2).

480   Additional changes to char composition, including organic P speciation and pH, also likely
481   contributed to decreased aqueous P mobilization with increased burning. We found a decrease in
482   non-molybdate reactive aqueous P, which is largely composed of organic P species (Condron et
483   al., 2015), with increasing burn severity (mixed effect model interaction term: $p < 0.001$, Fig. S6)
484   indicating less mobilization of organic P species with burning. The amount of mobilized P
485   compounds from char is also related to pH (Fig. 6), where less P compounds are released at
486   higher pH (Silber et al., 2010; Zheng et al., 2013). We found aqueous P mobilization had an
487   inverse relationship with pH for both Douglas-fir forest ($p < 0.001$; $r^2 = 0.45$) and sagebrush
488   shrubland ($p < 0.001$, $r^2 = 0.97$; Fig. 6). Overall, changing chemical composition of the charred

489   material decreases solubility and therefore reduces aqueous P mobilization into the environment
490   (Robinson et al., 2018; Uchimiya et al., 2015; Wu et al., 2023b; Xu et al., 2016).
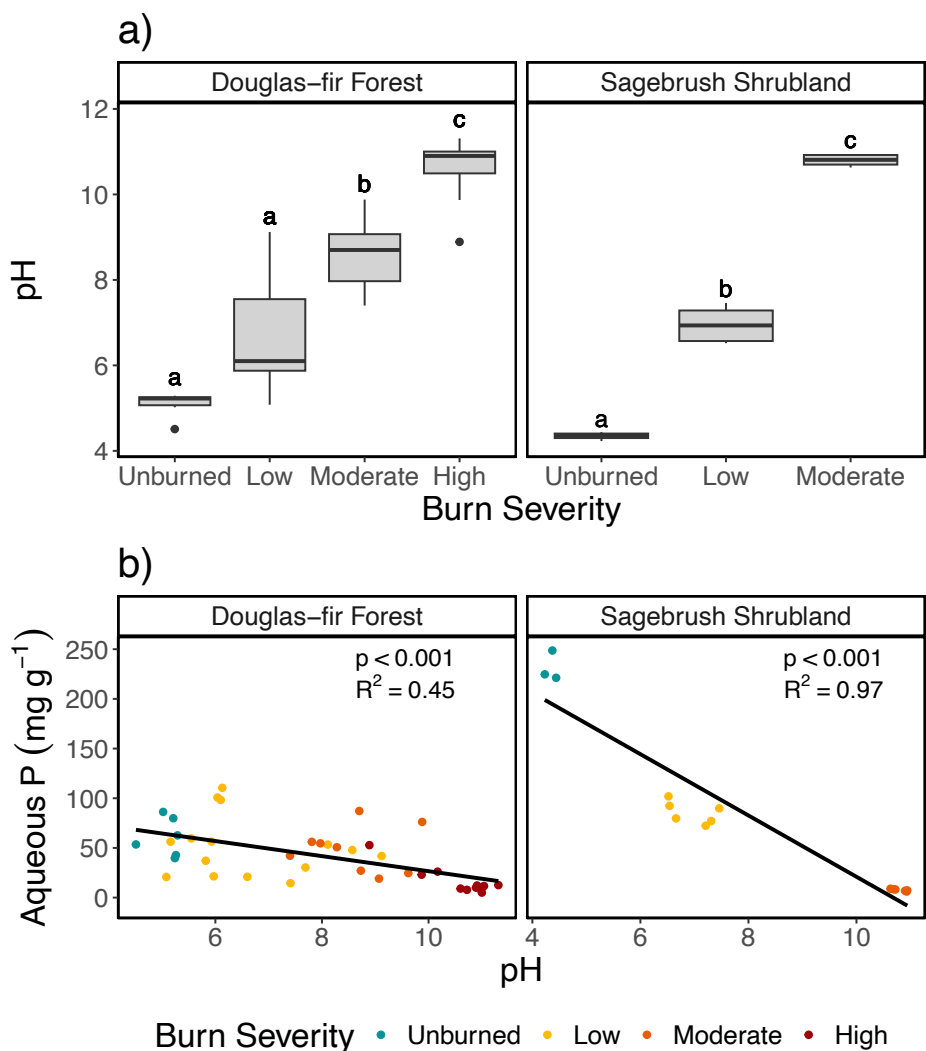

Figure 6. a) Boxplot of pH and burn severity. Letters denote post hoc findings of burn severity significant differences within a vegetation type, where the same lettering indicates no significant difference. See Table 1 for burn duration, temperature, and sample size. B) Relationship between pH and aqueous P for Douglas-fir forest and Sagebrush shrubland.

491   The extent of decreased aqueous P mobilization was vegetation dependent (interaction term of
492   mixed effect model; $p < 0.001$; Fig. 4). However, because both vegetation types had similar
493   percentages of Ca-P_i ($p = 0.18$; $r^2 = 0.15$), it indicates additional controls on aqueous P
494   mobilization. In addition to Ca-P_i and Mg-P_i, moderate-severity Douglas-fir forest contained P
495   compounds associated with Na (XANES: $22.7 \pm 22.1\%$) and organic P species (XANES: $6.9 \pm$
496   11.9%; NMR: $4.4 \pm 4.2\%$), whereas Na-P_i was not detected in sagebrush shrubland and organic
497   P was <1% (XANES: $0 \pm 0\%$; NMR: $0.7 \pm 0.4\%$; Figs. 2 and 3; Tables S2 and S4). Greater
498   solubility of these chemical species likely contributes to Douglas-fir forest moderate-severity
499   burns mobilizing 6.4 times more aqueous P than sagebrush shrubland ($p = 0.004$). Changing

16

chemical speciation from soluble organic and inorganic P to less soluble inorganic species (Li and Brett, 2013; Mukherjee and Zimmerman, 2013; Xu et al., 2016) resulted in the decreased export of P compounds with increased burn severity and contributed to the amount of P compounds mobilized from the respective vegetation types. This has important implications for P compounds that are transported in the environment because organic P can leach faster than many inorganic compounds (McDowell et al., 2021) and Na-P_i has been found as having high nutrient uptake and bioavailability (Li and Brett, 2013).

4 Conclusions

We found systematic changes in P chemistry across vegetation types; with increasing burn severity there were systematic shifts in P concentration and composition. We summarize our findings into a conceptual model to synthesize the main findings from this study (Fig. 7). From unburned to high-severity, identifiable structures decreased with increasing black charring and/or white ash (Fig. 7 panel 1; Fig. S1). Total Ca, Fe, Al, K, Ma, and Na concentrations increased (Table S5). Solid char concentration and composition controlled how P compounds were mobilized from burned material. Overall, burning resulted in an increase of char P concentration (Fig. 7 panel 1), which subsequently controlled the mobilization of particulate-bound P compounds from the chars. As burning progressed, chars compositionally transitioned from proportionally more organic P species, including both monoester and diesters, to Ca- and Mg-bound inorganic P species (Fig. 7 panel 1). These compositional changes resulted in less soluble inorganic P species and therefore reduced aqueous P mobilization in higher severity burns (Fig. 7 panel 2). Across vegetation types, chars became more divergent from the unburned vegetation material in P composition and mobilization potential as burning continued. Burn severity and vegetation type indirectly influenced the quantity and leachable phase (i.e., particulate or
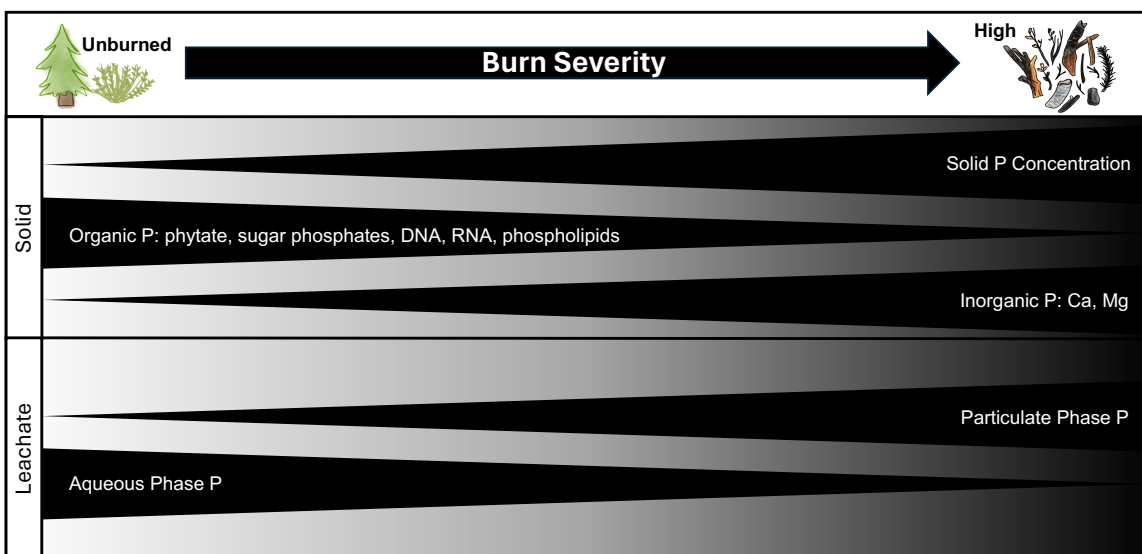

Figure 7. Conceptual framework for phosphorus biogeochemical shifts with increasing burn severity where solid P concentration increases, organic P species decrease while inorganic P increases. Leachates from the solid samples increased in mobilization of P in the particulate phase but decreased in aqueous P with burning.

524 aqueous) of P compounds that were mobilized from charred material by altering solid sample
525 concentration and composition.

526 Although both vegetation types followed similar concentration and compositional patterns,
527 sagebrush shrubland had greater P transformations than Douglas-fir forest across our P burn
528 severity conceptual model (Figs. 7 and S4). The P concentration of Douglas-fir forest chars and
529 leachates were more resilient to change with burning compared to sagebrush shrubland.
530 Phosphorus transformations in sagebrush shrubland moderate-severity burns generally
531 chemically resembled that of Douglas-fir forest high-severity burns (i.e., higher solid P
532 concentrations, more particulate leachable P, and more inorganic P). Taken together, this
533 indicates that although sagebrush shrubland experiences more low- and moderate-severity burns
534 than Douglas-fir forests (Stavi, 2019), the response of P chemistry in the environment post-fire
535 may resemble Douglas-fir forests burned at higher severities. This response is important to note
536 as shifts in fire severity are not occurring uniformly across all ecosystem types (Francis et al.,
537 2023; Halofsky et al., 2020; Reilly et al., 2017), which may influence post-fire P dynamics
538 across ecosystems.

539 The ultimate fate of P in the environment is determined by the interactions among biological,
540 chemical, physical and environmental factors (Condron et al., 2015; Yan et al., 2023). Our
541 leaching experiments provide insight to the potential mobilization mechanisms of P release from
542 solid vegetation chars. The key to bioavailable P is that it can enter solution for subsequent
543 uptake by plants and microbes (Kruse et al., 2015). We found burning resulted in less P released
544 into the environment in the aqueous phase, therefore, the differences in aqueous P we observed
545 with burn severity can influence biogeochemical cycling of P by altering its availability for
546 biological uptake and physical transport. The increase in particulate-bound P may be an
547 important source of available P over longer timeframes, compared to starting vegetation. For
548 instance, P mobilization into riverine systems can be long-lived following fire, altering P budgets
549 and aquatic ecosystem health (Bodí et al., 2014; Emmerton et al., 2020; Rust et al., 2018; Santín
550 et al., 2018; Silins et al., 2014). Our study helps to provide additional information on the
551 potential environmental fate of P post-fire in the context of different burn severities and
552 ecosystem types.

Acknowledgments

567 would like to give a special thanks to Erik Nelson, the beamline scientist from SSRL that helped
568 us collect those data.

Code/Data availability

570 All data and code are publicly available on the Environmental System Science Data
571 Infrastructure for a Virtual Ecosystem (ESS-DIVE) repository (Barnes et al., 2024; Grieger et al.,
572 2022) .

573

Competing interests

575 The authors declare no competing interests.

576

Author Contribution

578 Conceptualization: M.E.B., A.N.M.-P., J.A.R., K.D.B., E.B.G., S.G., T.D.S. Methodology and
579 Software: A.N.M.-P., M.E.B., S.G., J.D.B, K.B., E.B.G, P.A, V.A.G-C, K.M, J.A.R, R.P.Y.,
580 P.A.O., L.R. Investigation: M.E.B., P.A, S.G., K.M, L.R., J.A.R., J.D.B., K.D.B., R.P.Y. Data
581 Curation: M.E.B., S.G., P.A, V.A.G-C., A.N.M.-P., K.M, J.D.B., K.D.B., L.R., J.A.R. Formal
582 Analysis: M.E.B., A.N.M-P. J.A.R., V.A.G.-C., P.A., P.A.O., R.P.Y. Validation: M.E.B., P.A.,
583 K.M., V.A.G.-C., A.N.M-P., P.A.O., R.P.Y. Visualization: M.E.B., A.N.M.-P., S.G. Writing -
584 Original Draft: M.E.B., A.N.M.-P., J.A.R., S.G., K.M., R.P.Y. Writing – Review and Editing:
585 M.E.B., P.A., J.D.B., K.D.B., V.A.G.-C., E.B.G., A.N.M.-P., P.A.O., L.R., J.A.R, T.D.S., R.P.Y.

586

References

588 Ball, G., Regier, P., González-Pinzón, R., Reale, J., and Van Horn, D.: Wildfires increasingly
589 impact western US fluvial networks, Nat. Commun., 12, 2484, 2021.

590 Barnes, M. E., Aronstein, P. J., Bailey, J. D., Bladon, K. D., Forbes, B., Garayburu-Caruso, V.
591 A., Grieger, S., Graham, E. B., McKever, S. A., Myers, C. R., Munson, K. M., O'Day, P. A.,
592 Powers-McCormack, B., Renteria, L., Roebuck, A., Scheibe, T. D., Young, R. P., and Myers-
593 Pigg, A. N.: Data and scripts associated with: "Burn severity and vegetation type control
594 phosphorus concentration, molecular composition, and mobilization,"
595 https://doi.org/10.15485/2547035, 2024.

596 Bates, D., Mächler, M., Bolker, B., and Walker, S.: Fitting Linear Mixed-Effects Models Using
597 lme4, J. Stat. Softw., 67, 1–48, 2015.

598 Bird, M. I., Wynn, J. G., Saiz, G., Wurster, C. M., and McBeath, A.: The pyrogenic carbon
599 cycle, Annu. Rev. Earth Planet. Sci., 43, 273–298, 2015.

600 Blake, W. H., Theocharopoulos, S. P., Skoulikidis, N., Clark, P., Tountas, P., Hartley, R., and
601 Amaxidis, Y.: Wildfire impacts on hillslope sediment and phosphorus yields, J. Soils Sediments,
602 10, 671–682, 2010.

603 Bodí, M. B., Martin, D. A., Balfour, V. N., Santín, C., Doerr, S. H., Pereira, P., Cerdà, A., and
604 Mataix-Solera, J.: Wildland fire ash: Production, composition and eco-hydro-geomorphic effects,
605 Earth-Sci. Rev., 130, 103–127, 2014.

606 Bostick, K. W., Zimmerman, A. R., Wozniak, A. S., Mitra, S., and Hatcher, P. G.: Production
607 and Composition of Pyrogenic Dissolved Organic Matter From a Logical Series of Laboratory-
608 Generated Chars, Frontiers in Earth Science, 6, 43, 2018.

609 Brucker, C. P., Livneh, B., Minear, J. T., and Rosario-Ortiz, F. L.: A review of simulation
610 experiment techniques used to analyze wildfire effects on water quality and supply, Environ. Sci.
611 Process. Impacts, 24, 1110–1132, 2022.

612 Brucker, C. P., Livneh, B., Butler, C. E., and Rosario-Ortiz, F. L.: A laboratory-scale simulation
613 framework for analysing wildfire hydrologic and water quality effects, Int. J. Wildland Fire, 33,
614 https://doi.org/10.1071/wf23050, 2024.

615 Bünemann, E. K., Smernik, R. J., Marschner, P., and McNeill, A. M.: Microbial synthesis of
616 organic and condensed forms of phosphorus in acid and calcareous soils, Soil Biol. Biochem.,
617 40, 932–946, 2008.

618 Butler, O. M., Elser, J. J., Lewis, T., Mackey, B., and Chen, C.: The phosphorus-rich signature of
619 fire in the soil-plant system: a global meta-analysis, Ecol. Lett., 21, 335–344, 2018.

620 Cade-Menun, B. J.: Improved peak identification in 31P-NMR spectra of environmental samples
621 with a standardized method and peak library, Geoderma, 257–258, 102–114, 2015.

622 Cade-Menun, B. J., Berch, S. M., Preston, C. M., and Lavkulich, L. M.: Phosphorus forms and
623 related soil chemistry of Podzolic soils on northern Vancouver Island. II. The effects of clear-
624 cutting and burning, Can. J. For. Res., 30, 1726–1741, 2000.

625 Condron, L. M., Turner, B. L., and Cade-Menun, B. J.: Chemistry and dynamics of soil organic
626 phosphorus, in: Phosphorus: Agriculture and the Environment, American Society of Agronomy,
627 Crop Science Society of America, and Soil Science Society of America, Madison, WI, USA, 87–
628 121, 2015.

629 Dijkstra, F. A. and Adams, M. A.: Fire Eases Imbalances of Nitrogen and Phosphorus in Woody
630 Plants, Ecosystems, 18, 769–779, 2015.

631 Doerr, S. H. and Santín, C.: Global trends in wildfire and its impacts: perceptions versus realities
632 in a changing world, Philos. Trans. R. Soc. Lond. B Biol. Sci., 371,
633 https://doi.org/10.1098/rstb.2015.0345, 2016.

634 Doolette, A. L. and Smernik, R. J.: Phosphorus speciation of dormant grapevine (*Vitis vinifera*L.)
635 canes in the Barossa Valley, South Australia, Aust. J. Grape Wine Res., 22, 462–468, 2016.

636 Doolette, A. L., Smernik, R. J., and Dougherty, W. J.: Spiking improved solution phosphorus-31
637 nuclear magnetic resonance identification of soil phosphorus compounds, Soil Sci. Soc. Am. J.,
638 73, 919–927, 2009.

Elliott, K. J., Knoepp, J. D., Vose, J. M., and Jackson, W. A.: Interacting effects of wildfire severity and liming on nutrient cycling in a southern Appalachian wilderness area, Plant Soil, 366, 165–183, 2013.

Elser, J. J., Bracken, M. E. S., Cleland, E. E., Gruner, D. S., Harpole, W. S., Hillebrand, H., Ngai, J. T., Seabloom, E. W., Shurin, J. B., and Smith, J. E.: Global analysis of nitrogen and phosphorus limitation of primary producers in freshwater, marine and terrestrial ecosystems, Ecol. Lett., 10, 1135–1142, 2007.

Emmerton, C. A., Cooke, C. A., Hustins, S., Silins, U., Emelko, M. B., Lewis, T., Kruk, M. K., Taube, N., Zhu, D., Jackson, B., Stone, M., Kerr, J. G., and Orwin, J. F.: Severe western Canadian wildfire affects water quality even at large basin scales, Water Res., 183, 116071, 2020.

Fiddler, M. N., Thompson, C., Pokhrel, R. P., Majluf, F., Canagaratna, M., Fortner, E. C., Daube, C., Roscioli, J. R., Yacovitch, T. I., Herndon, S. C., and Bililign, S.: Emission factors from wildfires in the Western US: An investigation of burning state, ground versus air, and diurnal dependencies during the FIREX-AQ 2019 campaign, J. Geophys. Res., 129, https://doi.org/10.1029/2022jd038460, 2024.

Fischer, S. J., Fegel, T. S., Wilkerson, P. J., Rivera, L., Rhoades, C. C., and Rosario-Ortiz, F. L.: Fluorescence and Absorbance Indices for Dissolved Organic Matter from Wildfire Ash and Burned Watersheds, ACS EST Water, 3, 2199–2209, 2023.

Fox, J.: TEACHER'S CORNER: Structural Equation Modeling With the sem Package in R, Struct. Equ. Modeling, 13, 465–486, 2006.

Fox, J. and Weisberg, S.: An R Companion to Applied Regression, SAGE Publications, 608 pp., 2018.

Francis, E. J., Pourmohammadi, P., Steel, Z. L., Collins, B. M., and Hurteau, M. D.: Proportion of forest area burned at high-severity increases with increasing forest cover and connectivity in western US watersheds, Landsc. Ecol., 38, 2501–2518, 2023.

Galang, M. A., Markewitz, D., and Morris, L. A.: Soil phosphorus transformations under forest burning and laboratory heat treatments, Geoderma, 155, 401–408, 2010.

García-Oliva, F., Merino, A., Fonturbel, M. T., Omil, B., Fernández, C., and Vega, J. A.: Severe wildfire hinders renewal of soil P pools by thermal mineralization of organic P in forest soil: Analysis by sequential extraction and 31P NMR spectroscopy, Geoderma, 309, 32–40, 2018.

Glaser, B., Lehmann, J., and Zech, W.: Ameliorating physical and chemical properties of highly weathered soils in the tropics with charcoal – a review, Biol. Fertil. Soils, 35, 219–230, 2002.

Grieger, S., Bailey, J., Barnes, M., Bladon, K. D., Forbes, B., Garayburu-Caruso, V. A., Graham, E. B., Goldman, A. E., Homolka, K., McKever, S. A., Myers-Pigg, A., Otenburg, O., Renteria, L., Roebuck, A., Scheibe, T. D., and Torgeson, J. M.: Organic Matter Concentration and Composition of Experimentally Burned Open Air and Muffle Furnace Vegetation Chars across

676   Differing Burn Severity and Feedstock Types from Pacific Northwest, USA (V3),
677   https://doi.org/10.15485/1894135., 2022.

678   Gundale, M. J. and DeLuca, T. H.: Temperature and source material influence ecological
679   attributes of ponderosa pine and Douglas-fir charcoal, For. Ecol. Manage., 231, 86–93, 2006.

680   Halofsky, J. E., Peterson, D. L., and Harvey, B. J.: Changing wildfire, changing forests: the
681   effects of climate change on fire regimes and vegetation in the Pacific Northwest, USA, Fire
682   Ecology, 16, 4, 2020.

683   Hatch, L. E., Jen, C. N., Kreisberg, N. M., Selimovic, V., Yokelson, R. J., Stamatis, C., York, R.
684   A., Foster, D., Stephens, S. L., Goldstein, A. H., and Barsanti, K. C.: Highly Speciated
685   Measurements of Terpenoids Emitted from Laboratory and Mixed-Conifer Forest Prescribed
686   Fires, Environ. Sci. Technol., 53, 9418–9428, 2019.

687   Haugo, R. D., Kellogg, B. S., Cansler, C. A., Kolden, C. A., Kemp, K. B., Robertson, J. C.,
688   Metlen, K. L., Vaillant, N. M., and Restaino, C. M.: The missing fire: quantifying human
689   exclusion of wildfire in Pacific Northwest forests, USA, Ecosphere, 10, e02702, 2019.

690   Jolly, W. M., Cochrane, M. A., Freeborn, P. H., Holden, Z. A., Brown, T. J., Williamson, G. J.,
691   and Bowman, D. M. J. S.: Climate-induced variations in global wildfire danger from 1979 to
692   2013, Nat. Commun., 6, 7537, 2015.

693   Keeley, J. E.: Fire intensity, fire severity and burn severity: a brief review and suggested usage,
694   Int. J. Wildland Fire, 18, 116–126, 2009.

695   Kelly, S. D., Hesterberg, D., and Ravel, B.: Analysis of soils and minerals using X-ray
696   absorption spectroscopy, in: Methods of Soil Analysis Part 5—Mineralogical Methods,
697   American Society of Agronomy and Soil Science Society of America, Madison, WI, USA, 387–
698   463, 2015.

699   Kruse, J., Abraham, M., Amelung, W., Baum, C., Bol, R., Kühn, O., Lewandowski, H.,
700   Niederberger, J., Oelmann, Y., Rüger, C., Santner, J., Siebers, M., Siebers, N., Spohn, M.,
701   Vestergren, J., Vogts, A., and Leinweber, P.: Innovative methods in soil phosphorus research: A
702   review, J. Plant Nutr. Soil Sci. , 178, 43–88, 2015.

703   Lane, P. N. J., Sheridan, G. J., Noske, P. J., and Sherwin, C. B.: Phosphorus and nitrogen exports
704   from SE Australian forests following wildfire, J. Hydrol., 361, 186–198, 2008.

705   Lenth, R. V.: emmeans: Estimated marginal means, Github,
706   https://doi.org/10.1080/00031305.1980.10483031, 2023.

707   Li, B. and Brett, M. T.: The influence of dissolved phosphorus molecular form on recalcitrance
708   and bioavailability, Environ. Pollut., 182, 37–44, 2013.

709   Lopez, A. M., Avila, C. C. E., VanderRoest, J. P., Roth, H. K., Fendorf, S., and Borch, T.:
710   Molecular insights and impacts of wildfire-induced soil chemical changes, Nature Reviews Earth
711   & Environment, 5, 431–446, 2024.

712 Makarov, M. I., Haumaier, L., Zech, W., Marfenina, O. E., and Lysak, L. V.: Can 31P NMR
713 spectroscopy be used to indicate the origins of soil organic phosphates?, Soil Biol. Biochem., 37,
714 15–25, 2005.

715 McDowell, R. W., Worth, W., and Carrick, S.: Evidence for the leaching of dissolved organic
716 phosphorus to depth, Sci. Total Environ., 755, 142392, 2021.

717 McMeeking, G. R., Kreidenweis, S. M., Baker, S., Carrico, C. M., Chow, J. C., Collett, J. L., Jr,
718 Hao, W. M., Holden, A. S., Kirchstetter, T. W., Malm, W. C., Moosmüller, H., Sullivan, A. P.,
719 and Wold, C. E.: Emissions of trace gases and aerosols during the open combustion of biomass
720 in the laboratory, J. Geophys. Res. D: Atmos., 114, https://doi.org/10.1029/2009JD011836,
721 2009.

722 Merino, A., Jiménez, E., Fernández, C., Fontúrbel, M. T., Campo, J., and Vega, J. A.: Soil
723 organic matter and phosphorus dynamics after low intensity prescribed burning in forests and
724 shrubland, J. Environ. Manage., 234, 214–225, 2019.

725 Mishra, A., Alnahit, A., and Campbell, B.: Impact of land uses, drought, flood, wildfire, and
726 cascading events on water quality and microbial communities: A review and analysis, J. Hydrol.,
727 596, 125707, 2021.

728 Mukherjee, A. and Zimmerman, A. R.: Organic carbon and nutrient release from a range of
729 laboratory-produced biochars and biochar–soil mixtures, Geoderma, 193–194, 122–130, 2013.

730 Myers-Pigg, A. N., Grieger, S., Roebuck, J. A., Jr, Barnes, M. E., Bladon, K. D., Bailey, J. D.,
731 Barton, R., Chu, R. K., Graham, E. B., Homolka, K. K., Kew, W., Lipton, A. S., Scheibe, T.,
732 Toyoda, J. G., and Wagner, S.: Experimental Open Air Burning of Vegetation Enhances Organic
733 Matter Chemical Heterogeneity Compared to Laboratory Burns, Environ. Sci. Technol., 58,
734 9679–9688, 2024.

735 Noack, S. R., McLaughlin, M. J., Smernik, R. J., McBeath, T. M., and Armstrong, R. D.: Crop
736 residue phosphorus: speciation and potential bio-availability, Plant Soil, 359, 375–385, 2012.

737 Parsons, A., Robichaud, P., Lewis, S. A., Napper, C., and Clark, J. T.: Field guide for mapping
738 post-fire soil burn severity, United States Department of Agriculture Forest Service Rocky
739 Mountain Research Station, https://doi.org/10.2737/RMRS-GTR-243, 2010.

740 R Core Team: R: A Language and Environment for Statistical Computing, 2023.

741 Randerson, J. T., Chen, Y., van der Werf, G. R., Rogers, B. M., and Morton, D. C.: Global
742 burned area and biomass burning emissions from small fires, Biogeosciences, 117,
743 https://doi.org/10.1029/2012JG002128, 2012.

744 Ravel, B. and Newville, M.: ATHENA, ARTEMIS, HEPHAESTUS: data analysis for X-ray
745 absorption spectroscopy using IFEFFIT, J. Synchrotron Radiat., 12, 537–541, 2005.

746 Recena, R., Cade-Menun, B. J., and Delgado, A.: Organic phosphorus forms in agricultural soils
747 under Mediterranean climate, Soil Sci. Soc. Am. J., 82, 783–795, 2018.

748 Reilly, M. J., Dunn, C. J., Meigs, G. W., Spies, T. A., Kennedy, R. E., Bailey, J. D., and Briggs,
749 K.: Contemporary patterns of fire extent and severity in forests of the Pacific Northwest, USA
750 (1985–2010), Ecosphere, 8, e01695, 2017.

751 Robinson, J. S., Baumann, K., Hu, Y., Hagemann, P., Kebelmann, L., and Leinweber, P.:
752 Phosphorus transformations in plant-based and bio-waste materials induced by pyrolysis, Ambio,
753 47, 73–82, 2018.

754 Roebuck, J. A., Jr, Grieger, S., Barnes, M. E., Gillespie, X., Bladon, K. D., Bailey, J. D.,
755 Graham, E. B., Chu, R., Kew, W., Scheibe, T. D., and Myers-Pigg, A. N.: Molecular shifts in
756 dissolved organic matter along a burn severity continuum for common land cover types in the
757 Pacific Northwest, USA, Sci. Total Environ., 958, 178040, 2024.

758 Rose, T. J., Schefe, C., Weng, Z. (han), Rose, M. T., van Zwieten, L., Liu, L., and Rose, A. L.:
759 Phosphorus speciation and bioavailability in diverse biochars, Plant Soil, 443, 233–244, 2019.

760 Rust, A. J., Hogue, T. S., Saxe, S., and McCray, J.: Post-fire water-quality response in the
761 western United States, Int. J. Wildland Fire, 27, https://doi.org/10.1071/WF17115, 2018.

762 Saa, A., Trasar-Cepeda, M. C., Gil-Sotres, F., and Carballas, T.: Changes in soil phosphorus and
763 acid phosphatase activity immediately following forest fires, Soil Biol. Biochem., 25, 1223–
764 1230, 1993.

765 Santín, C., Doerr, S. H., Merino, A., Bucheli, T. D., Bryant, R., Ascough, P., Gao, X., and
766 Masiello, C. A.: Carbon sequestration potential and physicochemical properties differ between
767 wildfire charcoals and slow-pyrolysis biochars, Sci. Rep., 7, 11233, 2017.

768 Santín, C., Otero, X. L., Doerr, S. H., and Chafer, C. J.: Impact of a moderate/high-severity
769 prescribed eucalypt forest fire on soil phosphorous stocks and partitioning, Sci. Total Environ.,
770 621, 1103–1114, 2018.

771 Schaller, J., Tischer, A., Struyf, E., Bremer, M., Belmonte, D. U., and Potthast, K.: Fire enhances
772 phosphorus availability in topsoils depending on binding properties, Ecology, 96, 1598–1606,
773 2015.

774 Silber, A., Levkovitch, I., and Graber, E. R.: pH-dependent mineral release and surface
775 properties of cornstraw biochar: agronomic implications, Environ. Sci. Technol., 44, 9318–9323,
776 2010.

777 Silins, U., Bladon, K. D., Kelly, E. N., Esch, E., Spence, J. R., Stone, M., Emelko, M. B., Boon,
778 S., Wagner, M. J., Williams, C. H. S., and Tichkowsky, I.: Five-year legacy of wildfire and
779 salvage logging impacts on nutrient runoff and aquatic plant, invertebrate, and fish productivity,
780 Ecohydrol., 7, 1508–1523, 2014.

781 Smil, V.: PHOSPHORUS IN THE ENVIRONMENT: Natural Flows and Human Interferences,
782 Annu. Rev. Environ. Resour., 25, 53–88, 2000.

783 Son, J.-H., Kim, S., and Carlson, K. H.: Effects of Wildfire on River Water Quality and Riverbed
784 Sediment Phosphorus, Water Air Soil Pollut. Focus, 226, 26, 2015.

785 Souza-Alonso, P., Prats, S. A., Merino, A., Guiomar, N., Guijarro, M., and Madrigal, J.: Fire
786 enhances changes in phosphorus (P) dynamics determining potential post-fire soil recovery in
787 Mediterranean woodlands, Sci. Rep., 14, 21718, 2024.

788 Stavi, I.: Wildfires in Grasslands and Shrublands: A Review of Impacts on Vegetation, Soil,
789 Hydrology, and Geomorphology, Water, 11, 1042, 2019.

790 Sun, K., Qiu, M., Han, L., Jin, J., Wang, Z., Pan, Z., and Xing, B.: Speciation of phosphorus in
791 plant- and manure-derived biochars and its dissolution under various aqueous conditions, Sci.
792 Total Environ., 634, 1300–1307, 2018.

793 Turner, B. L., Cade-Menun, B. J., and Westermann, D. T.: Organic Phosphorus Composition and
794 Potential Bioavailability in Semi-Arid Arable Soils of the Western United States, Published in
795 Soil Sci. Soc. Am. J., 67, 1168–1179, 2003a.

796 Turner, B. L., Mahieu, N., and Condron, L. M.: Phosphorus-31 nuclear magnetic resonance
797 spectral assignments of phosphorus compounds in soil NaOH–EDTA extracts, Soil Sci. Soc.
798 Am. J., 67, 497–510, 2003b.

799 Turrion, M.-B., Lafuente, F., Aroca, M.-J., López, O., Mulas, R., and Ruipérez, C.:
800 Characterization of soil phosphorus in a fire-affected forest Cambisol by chemical extractions
801 and 31P-NMR spectroscopy analysis, Sci. Total Environ., 408, 3342–3348, 2010.

802 Uchimiya, M. and Hiradate, S.: Pyrolysis temperature-dependent changes in dissolved
803 phosphorus speciation of plant and manure biochars, J. Agric. Food Chem., 62, 1802–1809,
804 2014.

805 Uchimiya, M., Hiradate, S., and Antal, M. J., Jr: Dissolved Phosphorus Speciation of Flash
806 Carbonization, Slow Pyrolysis, and Fast Pyrolysis Biochars, ACS Sustainable Chem. Eng., 3,
807 1642–1649, 2015.

808 Method 365.3: Phosphorus, All Forms (Colorimetric, Ascorbic Acid, Two Reagent):
809 https://www.epa.gov/sites/default/files/2015-08/documents/method_365-3_1978.pdf.

810 Vega, J. A., Fontúrbel, T., Merino, A., Fernández, C., Ferreiro, A., and Jiménez, E.: Testing the
811 ability of visual indicators of soil burn severity to reflect changes in soil chemical and microbial
812 properties in pine forests and shrubland, Plant Soil, 369, 73–91, 2013.

813 Weihrauch, C. and Opp, C.: Ecologically relevant phosphorus pools in soils and their dynamics:
814 The story so far, Geoderma, 325, 183–194, 2018.

815 Werner, F. and Prietzel, J.: Standard Protocol and Quality Assessment of Soil Phosphorus
816 Speciation by P K-Edge XANES Spectroscopy, Environ. Sci. Technol., 49, 10521–10528, 2015.

Wu, H., Yip, K., Kong, Z., Li, C.-Z., Liu, D., Yu, Y., and Gao, X.: Removal and Recycling of Inherent Inorganic Nutrient Species in Mallee Biomass and Derived Biochars by Water Leaching, Ind. Eng. Chem. Res., 50, 12143–12151, 2011.

Wu, Y., Pae, L. M., Gu, C., and Huang, R.: Phosphorus Chemistry in Plant Ash: Examining the Variation across Plant Species and Compartments, ACS Earth Space Chem., https://doi.org/10.1021/acsearthspacechem.3c00145, 2023a.

Wu, Y., Pae, L. M., and Huang, R.: Phosphorus chemistry in plant charcoal: interplay between biomass composition and thermal condition, Int. J. Wildland Fire, 33, NULL-NULL, 2023b.

Xu, G., Zhang, Y., Shao, H., and Sun, J.: Pyrolysis temperature affects phosphorus transformation in biochar: Chemical fractionation and 31P NMR analysis, Sci. Total Environ., 569–570, 65–72, 2016.

Yan, Y., Wan, B., Jiang, R., Wang, X., Wang, H., Lan, S., Zhang, Q., and Feng, X.: Interactions of organic phosphorus with soil minerals and the associated environmental impacts: A review, Pedosphere, 33, 74–92, 2023.

Yu, F., Wang, J., Wang, X., Wang, Y., Guo, Q., Wang, Z., Cui, X., Hu, Y., Yan, B., and Chen, G.: Phosphorus-enriched biochar from biogas residue of Eichhornia crassipes: transformation and release of phosphorus, Biochar, 5, 82, 2023.

Yusiharni, E. and Gilkes, R.: Minerals in the ash of Australian native plants, Geoderma, 189–190, 369–380, 2012.

Zavala, L. M., De Celis, R., and Jordán, A.: How wildfires affect soil properties. A brief review, Cuad. Investig. Geogr., 40, 311–332, 2014.

Zheng, H., Wang, Z., Deng, X., Zhao, J., Luo, Y., Novak, J., Herbert, S., and Xing, B.: Characteristics and nutrient values of biochars produced from giant reed at different temperatures, Bioresour. Technol., 130, 463–471, 2013.

Zwetsloot, M. J., Lehmann, J., and Solomon, D.: Recycling slaughterhouse waste into fertilizer: how do pyrolysis temperature and biomass additions affect phosphorus availability and chemistry?, J. Sci. Food Agric., 95, 281–288, 2015.